Journal of Cleaner Production 549 (2026) 147864

Contents lists available at ScienceDirect

Journal of Cleaner Production

journal homepage: www.elsevier.com/locate/jclepro

Demonstration of a fertilizer-based liquid desiccant prototype for controlled plant environments

Sandeep Aryal [a,b], Foster Caragay [a], Danielle Monfet [c], Mark Lefsrud [d], Jonathan Maisonneuve [a,d,*]

[a] Department of Mechanical Engineering, Oakland University, Rochester, MI, United States
[b] Department of Engineering and Aviation Science, University of Maryland Eastern Shore, Princess Anne, MD, United States
[c] Département de Génie de la Construction, École de Technologie Supérieure, Montréal, QC, Canada
[d] Department of Bioresource Engineering, McGill University, Montreal, QC, Canada

HIGHLIGHTS

- First demonstration of fertilizer desiccant applied to a dynamic plant chamber.
- Fertilizer desiccant maintained relative humidity at setpoint of 60, 70 and 80 %.
- Maintained 60 % relative humidity throughout the 36-day growth cycle of arugula.
- Dehumidification matched peak plant loads with rates up to 0.76 ± 0.1 g/h.
- Shows an energy efficient way of managing humidity in closed plant environments.

GRAPHICAL ABSTRACT

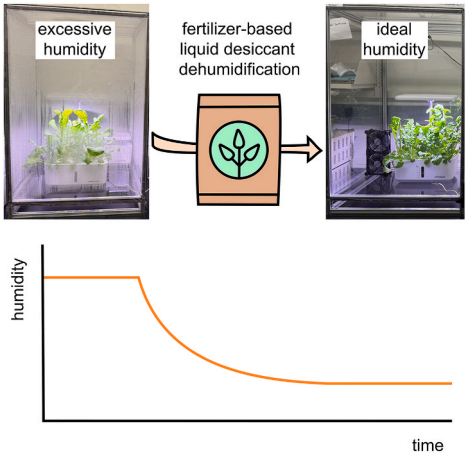

ARTICLE INFO

Keywords:
Controlled environment agriculture
Greenhouse
Dehumidification
Liquid desiccant

ABSTRACT

Healthy plant development and optimal crop yields require careful humidity control in closed plant environments. Recently, fertilizer solution has been proposed as an energy efficient liquid desiccant for greenhouse and plant environment applications. Here, we report the first demonstration of fertilizer-based solution being used to effectively control the humidity of a real and dynamic closed plant environment. This is done using a laboratory scale plant chamber and a liquid desiccant system with membrane contactors. Calcium nitrate solution is selected as a sample fertilizer and circulated in place of concentrated liquid desiccant. Hydroponic arugula is cultivated in the plant chamber. In the absence of any active dehumidification, humidity of the plant environment is shown to quickly approach saturation. Using the proposed fertilizer-based desiccant, humidity of the plant environment is successfully maintained at a variety of setpoints including 60, 70, and 80 % relative humidity with dehumidification rates reaching up to 0.76 ± 0.1 g/h. Testing is conducted under various conditions, including over all

* Corresponding author. Department of Bioresource Engineering, McGill University, Montreal, QC, Canada.
E-mail address: jonathan.maisonneuve@mcgill.ca (J. Maisonneuve).

https://doi.org/10.1016/j.jclepro.2026.147864
Received 8 September 2025; Received in revised form 19 January 2026; Accepted 23 February 2026
Available online 27 February 2026

stages of the plant growth cycle from germination to maturity, and stable humidity is confirmed throughout. Although not fully automated and integrated, these findings support the notion that fertilizer-based desiccant systems can be scaled and integrated for dehumidification and fertigation of controlled plant environments.

1. Introduction

World population has now surpassed 8 billion and may reach 10 billion by the year 2050 (Jain et al., 2023). This brings a pressing challenge to feed the world, as global food demand is expected to rise by more than 50 % over this period (van Dijk et al., 2021; Bahar et al., 2020). Already, about half of the world's vegetated land is used for agricultural food production, so simply expanding traditional farmland may risk deforestation or compromising sensitive ecosystems (Our World in Data, 2024). Sustainably feeding our growing population will therefore require innovation with our current farming practices.

One promising way of increasing food production is with controlled plant environments, including greenhouses, vertical farms, and indoor farms. In such environments, key parameters are optimized, such as light, temperature, humidity, and carbon dioxide levels. This enables reliable year-round crop production, independent of weather or season. Significantly greater productivity has been achieved in such systems, including reports of up to 12 × crop yields for tomato, pepper and lettuce (as compared to conventional field cultivation) (Cowan et al., 2022). Beyond increased food production, indoor farming offers several advantages such as reduced usage of pesticides and fertilizers, reduced water usage, improved food freshness and quality, and the potential to stabilize food prices (Penuela et al., 2024; Ampim et al., 2022; Stein, 2021). For these reasons, indoor farming is gaining market popularity throughout the world (Grand View Research, 2024).

One of the key conditions in the indoor plant environment is humidity. Due to plant evapotranspiration, moisture is continuously released into the indoor environment and if left uncontrolled, humidity can reach very high levels. For example, Fig. 1 shows an uncontrolled plant chamber in our laboratory, with condensation on the surfaces of the chamber clearly visible. Such high humidity can cause fungal disease, degrade crop health, reduce absorption of solar radiation, hinder plant transpiration and nutrient uptake, and ultimately compromise productivity (Tibbitts, 1979; Lysenko et al., 2023). Fig. 1 also shows the same laboratory plant chamber when humidity is properly controlled. For many common plant crops, the vapor pressure should be kept between 0.8 and 1.2 kPa below the dew point (Lu et al., 2015). This is known as the vapor pressure deficit, and is one of the key parameters that regulates evapotranspiration.

There are various ways of managing humidity in indoor plant systems including ventilation with or without heat recovery, heat pumps and mechanical refrigeration, and liquid or solid desiccant systems (Amani et al., 2020). Out of these, the simplest method is ventilation, wherein humid air is removed and replaced with fresh outdoor air. Such an approach is highly dependent on weather and involves a large energy cost since fresh air must be conditioned (Kittas and Bartzanas, 2007). Air-to-air heat exchangers can help to offset some of this energy cost by recovering sensible heat, but this still leaves the plant environment open to contamination by pests or pathogens (Zeng et al., 2017). For more carefully controlled closed environments, heat pumps and refrigeration are commonly used for dew-point dehumidification (Cheng and Zhang, 2023). This requires significant work (electricity) to power the compressor, and heat because air must commonly be re-heated to target indoor temperatures. More recently, liquid and solid desiccant materials have been adopted for moisture removal (Naik et al., 2020; Fahad et al., 2023; Luo and Yang, 2022). These require significant energy input because desiccant must be regenerated and then cooled but this can be cost effective if a low-grade heat source is available. In summary then, each of these technologies comes with its own advantages and disadvantages. Table 1 provides a summary of how these various technologies have been considered for application to controlled plant environments.

In recent years, we have advanced the novel concept of using

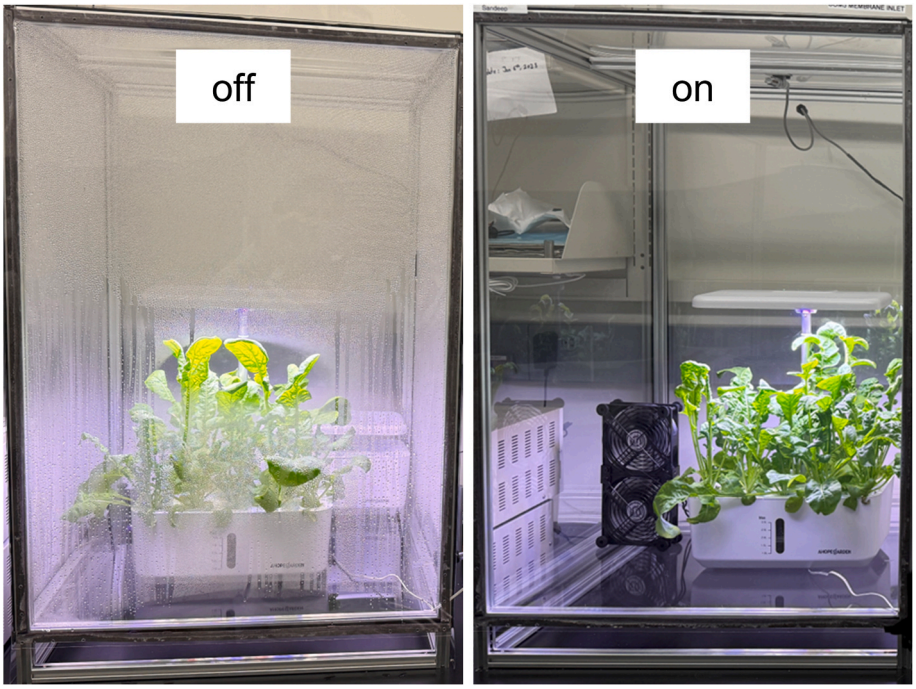

Fig. 1. Humidity control is an important part of creating an ideal plant environment. The image on the left shows a small plant chamber in our laboratory, operating without any humidity control, and high humidity can clearly be seen with condensation of the clear enclosure. The image on the right shows the same system with proper dehumidification.

Table 1
Studies conducted on dehumidification of indoor farming using different moisture removal technologies.

Investigators	Dehumidification technology	Study method	Crop
De Halleux and Gauthier (de Halleux and Gauthier, 1998)	Ventilation with heat recovery	Simulation	Tomato
Rousse et al. (Rousse et al., 2000)	Ventilation with heat recovery	Experimental	Tomato, cucumber
Chasseriaux et al. (Chasseriaux et al., 1987)	Heat pump	Theoretical	Tomato
Gilli et al. (Gilli et al., 2017)	Heat pump	Experimental	Cucumber
Sultan et al. (Sultan et al., 2015, 2016)	Solid desiccant	Experimental	Tomato, cucumber, lettuce, soybean
Ali et al. (Ali et al., 2017)	Liquid desiccant	Theoretical	n/a
Bettahalli et al. (Bettahalli et al., 2016)	Liquid desiccant	Experimental and theoretical	n/a
Ganguly and Gosh (Ghosh and Ganguly, 2017)	Liquid desiccant	Experimental and theoretical	Cucumber and lettuce
Lefers et al. (Lefers et al., 2018, 2019)	Liquid desiccant	Experimental	n/a
Lynchos and Davies (Lychnos and Davies, 2012)	Liquid desiccant	Experimental and simulation	Lettuce

fertilizer solution to drive dehumidification of controlled plant environments (Moussaddy et al., 2022, 2024). The basic concept is illustrated in Fig. 2(a). At high concentrations, the vapor pressure of fertilizer solution is less than that of the humid plant environment. As such, fertilizer solution can behave as a liquid desiccant, drawing water vapor from the humid air to condense on the surface of the solution. To accelerate dehumidification, the contact area between the two fluids can be maximized with a variety of common liquid desiccant delivery methods, such as spray, falling film, packed bed, or as shown here, across a vapor selective membrane (Sadasivam and Balakrishnan, 1991; Gurubalan and Simonson, 2021). As fertilizer solution is diluted by water vapor over time, a chiller is used to slightly cool the solution and maintain dehumidification performance. Finally, when concentration is reduced to levels that are acceptable for plants, the fertilizer can be used directly for fertigation, effectively combining dehumidification and nutrient delivery into a single, energy-efficient process (Moussaddy et al., 2024). The major advantage of fertilizer-based desiccants is then that it eliminates the need for energy intensive regeneration, as required by conventional liquid or solid desiccants. The underlying psychrometric principles governing the operation of the fertilizer-based liquid desiccant are illustrated in Fig. 2(b). These principles are not unique to fertilizer solutions; the same psychrometric framework applies broadly to traditional liquid desiccant systems, where moisture transfer is driven by the vapor pressure difference between air and the desiccant and can be regulated through desiccant concentration and temperature.

So far, in our previous work on this subject we have successfully validated the concept showing dehumidification with a variety of common fertilizer solution (Moussaddy et al., 2022). We have also evaluated the process' energy efficiency, achieving specific energy use as low as 0.29 kWh work per kg of vapor removal, showing that it compares very well with other dehumidification technologies and standards (Aryal et al., 2025). However, to this date, fertilizer-based liquid desiccants have not actually been applied to a controlled plant environment. The scope of this study is therefore to demonstrate the operation of a fertilizer-based liquid desiccant dehumidification system when it is integrated with a real plant chamber. The paper begins by

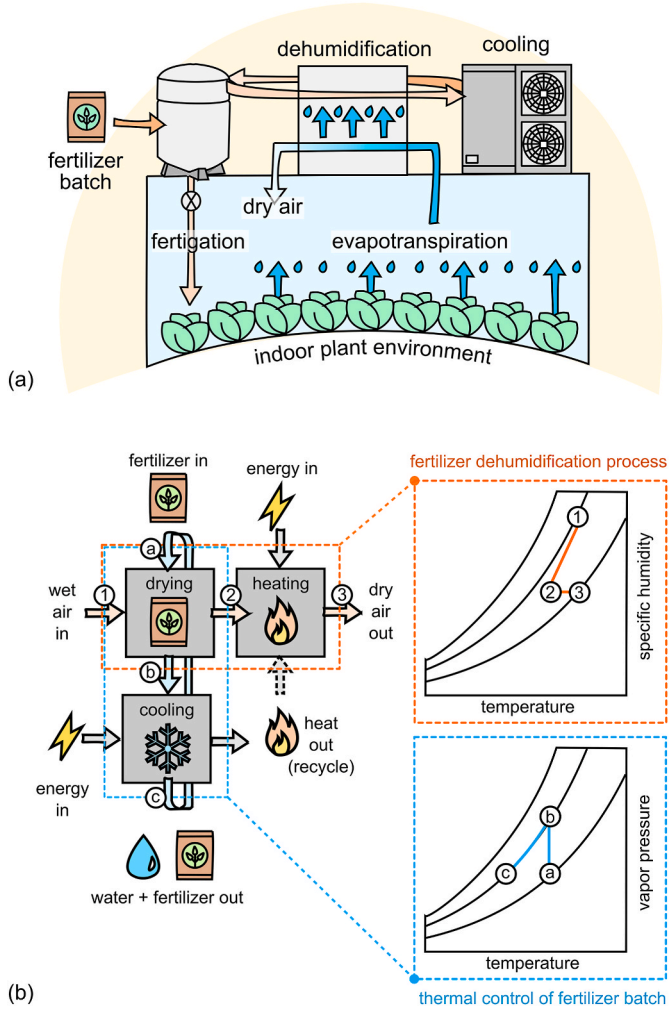

Fig. 2. (a) In the proposed dehumidification system, concentrated fertilizer solution is used in place of traditional liquid desiccants. Water vapor is transferred from the humid plant environment to the liquid desiccant, driven by the vapor pressure difference between the two. Liquid desiccant is cooled to ensure consistent dehumidification performance as the batch of fertilizer is diluted. After sufficient time, fertilizer solution can be delivered to the plants, as intended, to provide nutrients for plant growth. (b) Psychrometric principles of the fertilizer-based dehumidification system. (1)-(2): Moisture is absorbed by the cooled fertilizer liquid desiccant, reducing air humidity and slightly lowering air temperature. (2)-(3): The air is reheated to ambient conditions using a heat pump or available waste heat. (a)-(b): Water vapor absorption dilutes the fertilizer solution, decreasing its concentration and increasing its vapor pressure. (b)-(c): The diluted fertilizer solution is cooled to re-establish the target vapor pressure.

describing the plant chamber that has been developed in our laboratory. The plant chamber includes a commercial hydroponic grow system that is used for cultivation of arugula throughout the study. Then, the dehumidification apparatus is described, which includes a series of hollow fiber membrane modules across which water vapor is transferred from the humid air to the concentrated fertilizer. A simple illustration of the prototype is provided in Fig. 3. Test conditions and methods of analysis are described. Finally, results are included, showing dehumidification for a number of test trials with plant crops at different stages, kept at different humidity levels. Ultimately, the contribution of this work to the scientific literature is the first demonstration of fertilizer solution being used to control humidity of a real plant growth chamber. The successful demonstration of this represents an important step forward in enabling energy efficient dehumidification for controlled plant environments.

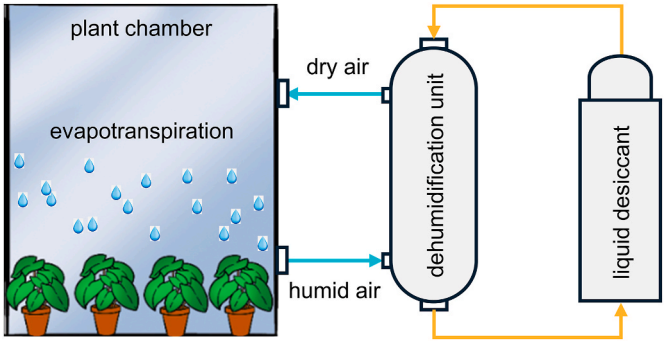

Fig. 3. Closed plant environment and dehumidification unit used to demonstrate dehumidification with fertilizer-based liquid desiccants.

2. Materials and methods

2.1. Hydroponic plant chamber

A laboratory scale plant chamber was designed and fabricated as shown in Fig. 5(a). The chamber is made of anodized 2020 aluminum extrusion rails for framing (IXGNIJ, Dongguan, China) with transparent plexiglass for glazing (Duco Plus, Warminster, PA) and has overall dimensions of 24 × 24 × 34 inches. The chamber contains of a commercial hydroponic grow system (Ahopegarden, Guangzhou, China). The hydroponic system has a 3-L capacity for hydroponic solution that is aerated and mixed by a small internal pump, as well as 10 pods that can accommodate conical sponge inserts used to promote germination and root development. The pods are shown in Fig. 4(b). The hydroponic system includes a full spectrum LED grow light that is maintained at 14 inches above the base. Air from the plant chamber is circulated towards an external dehumidification unit before being returned to the chamber, where temperature and humidity are monitored by a sensor (AM2315, Aosong Electronics, Guangzhou, China). A 12 V, 1.2 W fan (ELUTENG, ShenZhen Engesen Electronics, Shenzhen, China) operates continuously in the plant chamber to ensure that the microclimate is evenly mixed.

2.2. Liquid desiccant dehumidification system

Air is drawn from the plant chamber and directed towards an external dehumidification unit using a 12 V diaphragm air pump (SEAFLO 21 Series, Xiamen, China). Air flow rate is regulated using a mass flow controller (GFC17, Aalborg, Orangeburg, NY). The temperature and humidity of air are measured at the inlet (when air is removed from the plant chamber) and at the outlet (prior to returning air to the plant chamber) using capacitive sensors (AM2315, Aosong Electronics, Guangzhou, China). Inlet and outlet pressures are also measured with a pressure transducer (GC557F0142CD, Ashcroft, Stratford, CT). Since dehumidification performance is sensitive to pressure, a pressure regulator is installed at the air outlet to ensure that both air and desiccant are at equal applied pressure in the dehumidification unit.

The external dehumidification unit is shown in Fig. 5 and additional renderings are included in Supplementary Note 1. As shown, the system featured two hollow fiber membrane modules (PDMSXA-1.0, PermSelect, Ann Arbor, MI) that are placed in parallel to increase contact area and dehumidification capacity. Each module includes five ports, enabling a counterflow configuration where warm, humid air flows through the lumens and cold fertilizer desiccant solution circulates through the shell side. Additional membrane specifications are provided in Section 2.3. A positive displacement diaphragm pump (SFDP1-030-045-33, Seaflo, Xiamen, China) is used to draw liquid desiccant from a 3 L reservoir and circulate it through the membrane modules. The flow rate is monitored using a mass flow meter (8051K107, McMaster-Carr, Elmhurst, IL) and controlled by adjusting the DC voltage supply to the pump. To dampen any flow pulsations and reduce vibration, an inline accumulator tank (SFAT-075-125-01, Seaflo, Xiamen, China) is included. Liquid desiccant is cooled before entering the membrane modules using a stacked plate heat exchanger (35115K62, McMaster-Carr, Elmhurst, IL) that receives chilled water from a thermostatically controlled bath (TC550-SD, Brookfield, Middleboro, MA). Desiccant temperatures at the membrane inlets and outlets are tracked using inline thermal resistance sensors (800-32/140-1188, Noshok, Berea, OH) housed within protective thermowells (75-025-316SS, Noshok, Berea, OH). Desiccant pressure at the membrane inlet is also monitored with a pressure transducer (GC557F0142CD, Ashcroft, Stratford, CT). All desiccant lines are insulated with foam tubing to minimize heat gain from the ambient environment.

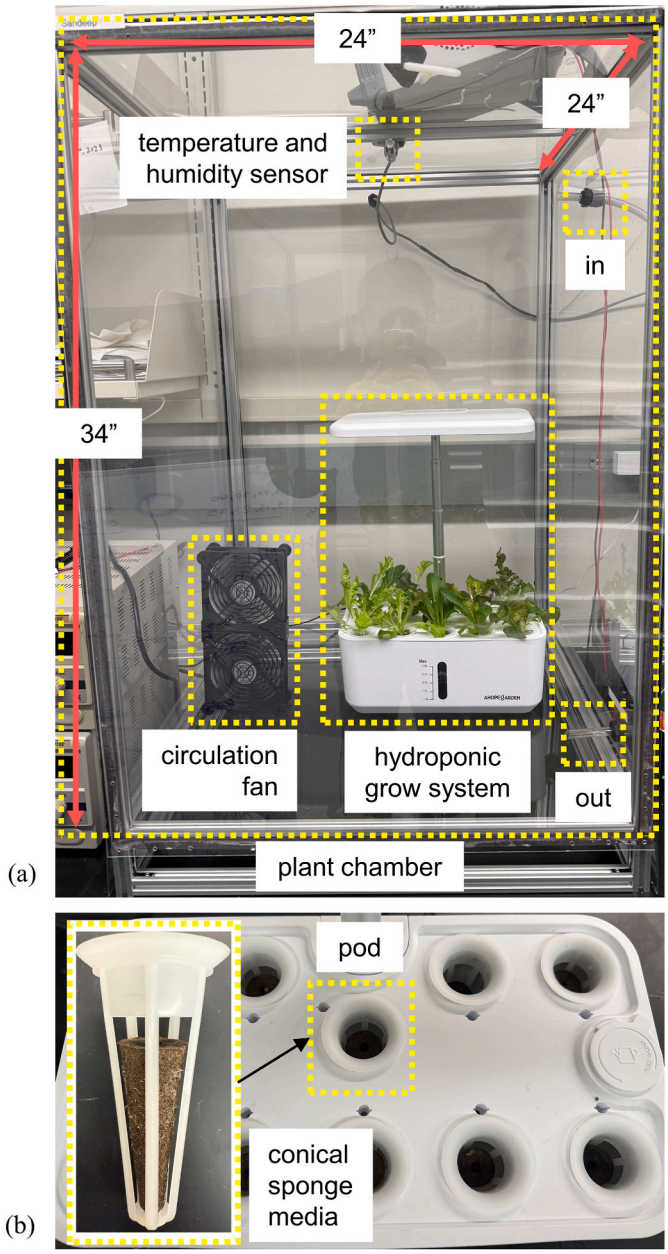

Fig. 4. (a) Custom plant chamber with hydroponic grow system. The unit measures 24 × 24 × 34 inches and is equipped with a fan for air circulation, temperature and humidity sensors, and ports for circulating air to an external dehumidification unit. (b) The hydroponic system has a volume capacity of 3 L and can accommodate up to 10 plants grown in conical sponge media that is submerged in the hydroponic solution.

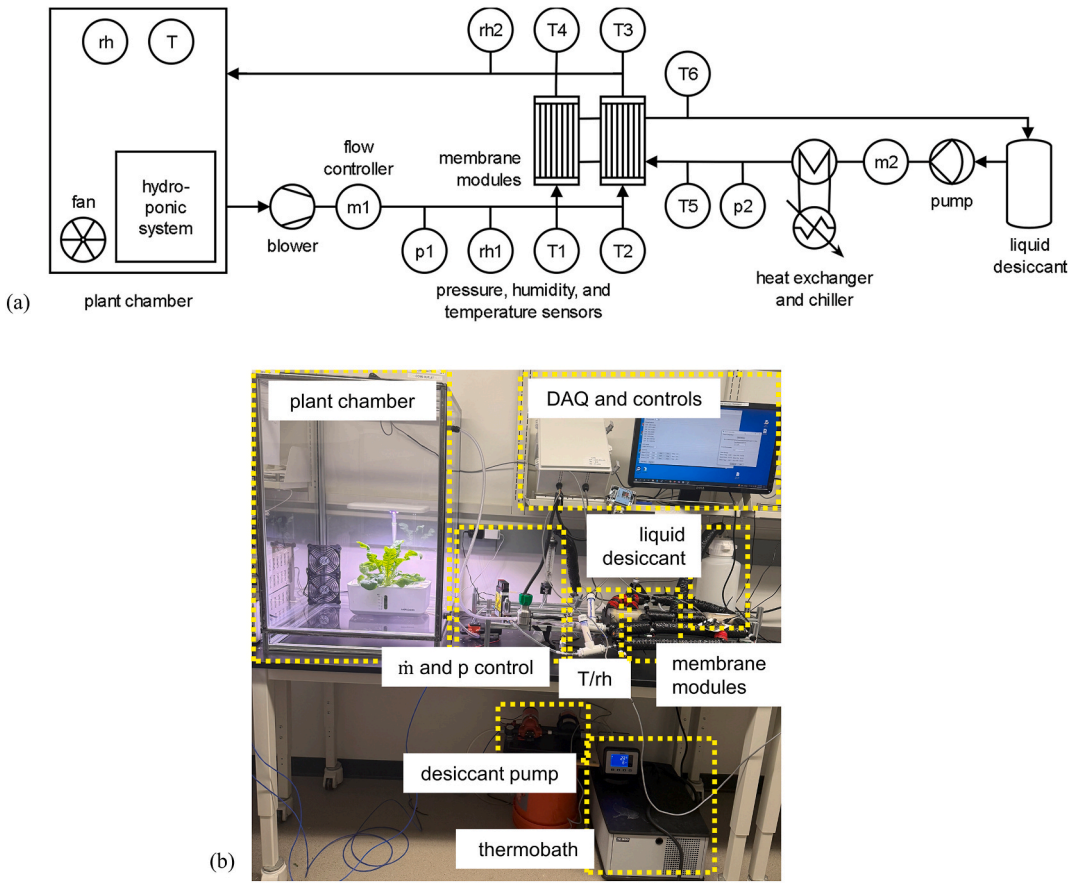

Fig. 5. (a) Schematic and (b) picture of the laboratory-scale liquid desiccant dehumidification system. In this study, concentrated fertilizer solution is used as the liquid desiccant. Air is circulated from the plant chamber to the dehumidification unit in order to control humidity. Instrument numbers are listed in Table 2 with key specifications.

Table 2 provides a summary of all sensors and instrumentation included in the plant chamber and desiccant dehumidification system, with their key specifications including full scale and uncertainty. Instrument numbers corresponde to locations indicated in Fig. 5.

2.3. Membrane module

For this study, two commercial membrane modules placed in parallel were selected as the core component of the dehumidification process. Each module includes 12,600 dense hollow fiber membranes made from dense polydimethylsiloxane, providing a total surface area of 2 m^2 across which water vapor is driven by the vapor pressure difference between humid air and concentrated desiccant. It should be noted that other methods of bringing air and liquid desiccant into contact could also be used in this place (e.g., spray, falling film, packed bed). Air is circulated through the membrane hollow fibers, while the liquid desiccant is circulated around these fibers on the shell side of the module in a counter flow arrangement. Fig. 6 shows an image of the membrane fibers captured with a scanning electron microscope (JSM 6510, Jeol, Peabody, MA). Key membrane specifications are listed in Table 3.

2.4. Data analysis

Performance of the dehumidification system was evaluated in terms of several key metrics. First, the relative humidity *rh* and temperature *T* of the plant chamber were directly observed. For reference, the associated vapor pressure p_{H2O} can be easily calculated and compared to the saturation pressure p_{sat}, which can be obtained from the empirical Magnus-Tetens equation shown in equation (2) (where p_{sat} is in Pa and *T* is in ^{o}C) (Xu et al., 2012). For convenience, the difference between these two can also be expressed as the vapor pressure deficit *VPD*.

$$p_{H2O} = rh\ p_{sat} \quad (1)$$

Table 2
Sensor and instrumentation specifications.

Instrument	Manufacturer	Model number	Full scale ± Uncertainty	Instrument number
Air feed				
Mass flow controller	Aalborg	GFC17	5 ± 0.05 SLPM	m1
Resistive temperature detector	TWTADE	MT-6340-30	200 ± 0.5 °C	T1, T2, T3, T4
Capacitive humidity and temperature sensor	Aosong Electronics	AM2315	100 ± 2 %	rh1, rh2
Pressure transducer	Ashcroft	GC557F0142CD	75 ± 0.38 psi	p1
Liquid desiccant				
Mass flow meter	McMaster-Carr	8051K107	1.6 ± 0.05 GPM	m2
Thermal resistance sensor	Noshok	800-32/140-1188	60 ± 0.3 °C	T5, T6
Pressure transducer	Ashcroft	GC557F0142CD	75 ± 0.38 psi	p2

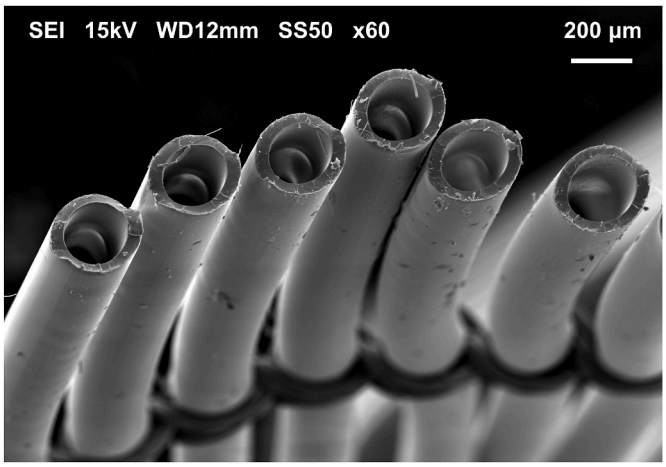

Fig. 6. SEM image of membrane hollow fibers at 60 × magnification.

Table 3
Membrane specifications.

Material	Polydimethylsiloxane
Module type	Hollow fiber
Membrane area	1 m^2
Fiber length	0.14 m
Fiber diameter (outer)	300×10^{-6} m
Fiber thickness	55×10^{-6} m
Number of fibers	12,600
Flow orientation	Counter flow

$$p_{sat} = 613.87 \exp\left(\frac{17.50\ T}{241.2 + T}\right) \quad (2)$$

$$VPD = p_{sat} - p_{H2O} = p_{sat}\,(1 - rh) \quad (3)$$

Second, the rate of dehumidification $\dot{m}_{dehumidification}$ achieved by the fertilizer desiccant system was experimentally evaluated. This was done by taking a mass balance of the humid air at the dehumidification unit's inlet and outlet. Supplementary Note 2 provides a detailed derivation of how equation (4) can be obtained from the difference between inlet and outlet water vapor and then related to pressure and humidity sensors that are mounted on the bench. As a measure of the membrane performance (or as an indication of how effectively the membrane area is utilized), the rate of dehumidification can also be normalized over the membrane surface area A to obtain vapor flux J.

$$\dot{m}_{dehumidification} = \dot{m}\left(\left(\frac{rh\ p_{sat}}{p - rh\ p_{sat}}\right)_{in} - \left(\frac{rh\ p_{sat}}{p - rh\ p_{sat}}\right)_{out}\right)\frac{M_{H2O}}{M_{air}} \quad (4)$$

$$J = \dot{m}_{dehumidification}/A \quad (5)$$

Where $\dot{m}$ is the circulation rate of air, p is the air pressure, and M is the molar mass.

For reference, the dehumidification rate can also be compared to the plant evapotranspiration rate $\dot{m}_{evapotranspiration}$. This can be calculated from the change in water vapor content that is observed over some discrete time interval $\Delta t = t_2 - t_1$ in the plant chamber, and by accounting for water vapor that is removed by dehumidification. From equation (6) it follows that when there is no change in humidity in the plant chamber $\dot{m}_{evapotranspiration} = \dot{m}_{dehumidification}$.

$$\dot{m}_{evapotranspiration} = \frac{\Delta m}{\Delta t} + \dot{m}_{dehumidification} \quad (6a)$$

$$\dot{m}_{evapotranspiration} = \frac{\rho_{air}\ V}{t_2 - t_1}\left(\left(\frac{rh\ p_{sat}}{p - rh\ p_{sat}}\right)_2 - \left(\frac{rh\ p_{sat}}{p - rh\ p_{sat}}\right)_1\right)\frac{M_{H2O}}{M_{air}} + \dot{m}_{dehumidification} \quad (6b)$$

Where ρ is density and V is the volume of the plant chamber.

Supplementary Note 3 provides sample calculations to illustrate dehumidification analysis from equations (1)–(6) with the associated propagation of experimental uncertainty.

2.5. Test conditions

Three sets of tests were completed to evaluate the proposed fertilizer-based liquid desiccant dehumidification system under a range of conditions. Table 4 provides a summary of all test conditions.

In the first set of tests, all hydroponic pods were seeded with arugula (*Eruca sativa*, Johnny's Selected Seeds, Winslow, ME) which was grown to maturity (~36 days). Plants were provided a commercial two-part nutrient blend (Ahopegarden, Guangzhou, China) with composition specified in Table 5. Plants were grown with a 16-h photoperiod with daily light integral (DLI) value of 13 mol/m^2/day. Once plants reached maturity, conditions of the plant chamber (including temperature, relative humidity, vapor pressure deficit, and evapotranspiration rates) were observed in the absence of any dehumidification control. The objective of this testing was to characterize the passive response of the plant chamber and evaluate the maximum dehumidification load.

In the second round of tests, the fertilizer dehumidification system was switched on to confirm its capacity for reducing indoor humidity to target levels of 60, 70, and 80 %. These humidity targets were achieved by regulating the liquid desiccant temperature and manually operating the dehumidification system's duty cycle. Throughout this round of tests, super concentrated calcium nitrate tetrahydrate $Ca(NO_3)_2{\cdot}4H_2O$ (99 % purity, Fisher Scientific, Hampton, NH) at 1000 g/l was used as liquid desiccant and circulated at a rate of 2 lpm and pressure of 18 psia. Of note, for the purpose of these experiments, the hydroponic plant system continued to be provided with the two-part nutrient blend, rather than the concentrated nitrogen fertilizer, as intended. In other words, the same fertilizer solution was not used for both fertigation and dehumidification in the present study because the existing hydroponic system was not adapted to allow bidirectional fluid circulation, as would be required for both operations. Also, there are questions about membrane fouling and fertilizer precipitation, which must be further investigated before fertilizer desiccant can be fully integrated with the plant nutrient

Table 4
Test conditions for the fertilizer-based desiccant dehumidification system.

	Round 1	Round 2	Round 3
	no dehumidification	short tests	extended tests
Hydroponic System			
Plant crop	arugula (*Eruca sativa*)	arugula (*Eruca sativa*)	arugula (*Eruca sativa*)
Photoperiod	16 h	16 h	16 h
Nutrient solution	1.5 mL/day	1.5 mL/day	1.5 mL/day
Plant stage	day 21	day 21	days 1-36
Dehumidification System			
Humidity setpoint	n/a	60, 70, 80 % rh	60 % rh
Air circulation rate	n/a	1.5-2 sL/min	1.5-2 sL/min
Air pressure	n/a	1 atm	1 atm
Desiccant circulation rate	n/a	2 L/min	2 L/min
Desiccant pressure	n/a	1.2 atm	1.2 atm
Desiccant temperature	n/a	2-7 °C	3-5 °C
Fertilizer desiccant	n/a	$Ca(NO_3)_2{\cdot}4H_2O$	$Ca(NO_3)_2{\cdot}4H_2O$
Desiccant concentration	n/a	1000 g/l	25 g/l

Table 5
Nutrient composition of commercial fertilizer blend supplied to plants.

Solution A	(%)
N	8.5
Soluble P_2O_5	7.5
K_2O	29.5
Mg	2.5
EDTA-Fe	0.3
EDTA-Mn	0.06
EDTA-Cu	0.005
EDTA-Zn	0.01
Solution B	
Total N	11
CaO	25

supply.

Finally, in the third round of testing, the dehumidification system was operated throughout all stages of the plant development, from germination to maturity, in order to observe dehumidification performance. Due to limited capacity of the dehumidification system, only two of the hydroponic pods were seeded with arugula (*Eruca sativa*, Johnny's Selected Seeds, Winslow, ME). Plants were grown under similar conditions reported above. Calcium nitrate tetrahydrate $Ca(NO_3)_2{\cdot}4H_2O$ (99 % purity, Fisher Scientific, Hampton, NH) was again used as the fertilizer-based desiccant, but was limited to a concentration of 25 g/l. This concentration was selected to be more representative of the diluted fertilizer that can be expected in real applications, given that such plants only require about ~15 g/plant to complete their growth cycle. It is not intended to represent a long-term desiccant state, but rather the terminal condition of the operating window, corresponding to a nutrient solution that is safe and representative for plant uptake.

3. Results

3.1. Response of the plant system without dehumidification

The first round of testing was done to characterize the response of the plant system in the absence of any dehumidification. Fig. 7 shows the resulting plant environment over a sample period of 96 h (4 days) when hydroponic arugula is growing. At this stage, the plants were fully-mature with a dense, well-developed leafy canopy, as shown in the image.

The daily cycle was clearly driven by the photoperiod which includes a 16-h light period and an 8-h dark period, as marked on the figure. As shown, temperature increases from 21.4 ± 0.2 °C at the start of the day to a peak of 23.3 ± 0.2 °C, and humidity likewise from 62 ± 2 % to near saturation at its peak. Such a cyclical, daily response is expected and is characteristic of plant systems. During light periods, stomata open, increasing transpiration, and releasing moisture into the environment. Conversely, stomata close during dark periods, reducing transpiration, and a drop in humidity is observed as some humidity is taken up by the plant and some condenses.

Fig. 7 also shows the vapor pressure deficit in the plant environment and the resulting rate of evapotranspiration that it causes. Evapotranspiration peaked at the start of each day, when the vapor pressure deficit is at its highest and when lighting is first switched on. The maximum rate of evapotranspiration is useful to note as it provides a measure of the dehumidification capacity that is needed for the liquid desiccant system, which is important for sizing. The maximum rate of dehumidification observed during these tests is 1.39 ± 0.08 g/h, which occurs when the vapor pressure deficit is 1.0 ± 0.6 kPa. For reference, a vapor pressure deficit between 0.8 and 1.2 kPa is generally considered ideal for vegetative plant growth (Cutress, 2021). Also, for comparison, the evapotranspiration rate can be expressed on a per plant unit, which gives 0.139 ± 0.008 g/h/plant for the previously mentioned maximum. Or it

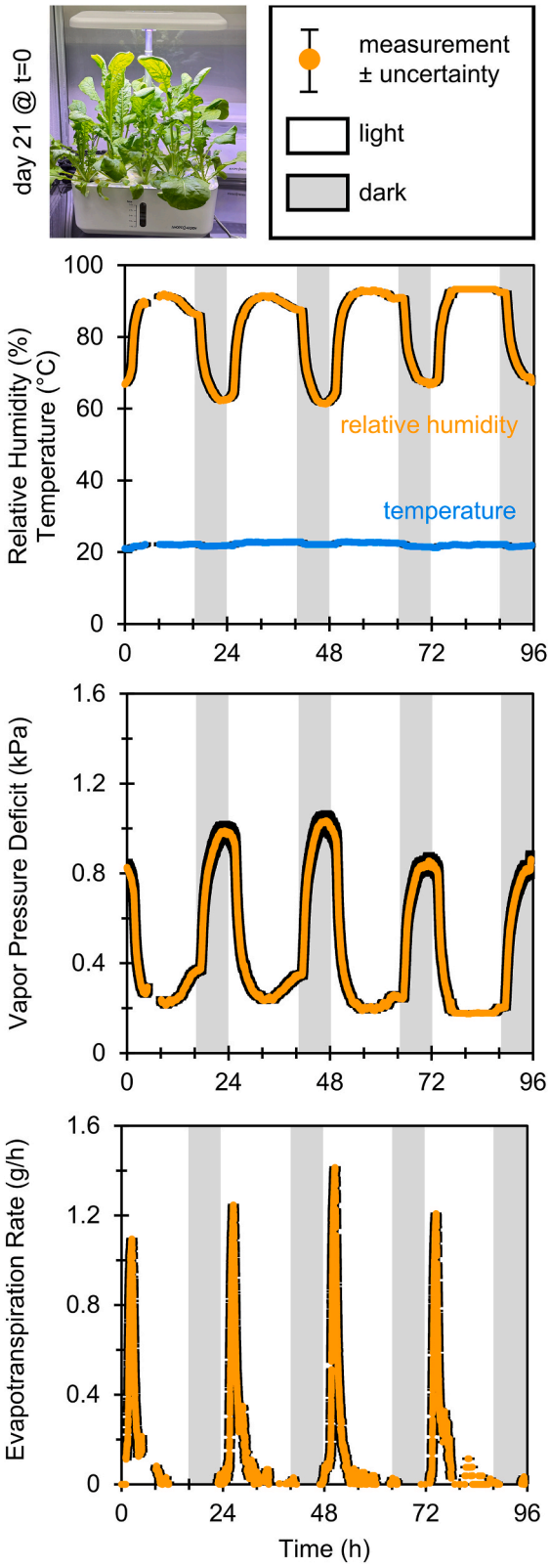

Fig. 7. Temperature (a), humidity (a), vapor pressure deficit (b) and evapotranspiration rate (c) inside the mini greenhouse chamber for a period of 96 h with fully grown arugula at its mature stage (day 21 after germination). Relative humidity and vapor pressure show clear diurnal fluctuations driven by plant evapotranspiration. No dehumidification system was used during this period.

can be expressed per unit of grow space, which gives 48.1 ± 2.8 g/h/m^2. These values compare reasonably well with evapotranspiration rates reported in the literature, which range from 0.1 to 0.8 g/h/plant for fully-developed arugula (Marangoni et al., 2019).

3.2. Dehumidifying the plant chamber with fertilizer-based desiccant

In the second round of testing, the dehumidification system was switched on to verify the capacity of the fertilizer-based liquid desiccant to manage humidity at a range of setpoints, including 60, 70, and 80 % relative humidity. These tests were conducted with the hydroponic system at full capacity, including 10 fully-developed arugula plants (day 21), and under light conditions. Calcium nitrate solution near its solubility limit was selected as the fertilizer desiccant.

Fig. 8 shows the results and confirms successful dehumidification of the plant system. The fertilizer-based liquid desiccant was able to effectively maintain stable humidity within 2.3 % of each of the setpoints. After successfully maintaining humidity for a period of approximately 60 min, the dehumidification system was then switched off to observe the response of the system for an additional period. As shown, humidity steadily increased, nearing saturation after about 60 min.

During operation, the dehumidification rate ranged from 0.46 to 0.70 ± 0.08 g/h, with the higher values required to maintain a drier environment. For reference, the evapotranspiration rate is also shown. During the period when the dehumidification system is on and humidity is held constant, we expect the evapotranspiration rate to be nearly equal to the dehumidification rate. This was mostly true, except that the plot for evapotranspiration is noisy, as it is very sensitive to small but sudden changes in the humidity sensor output. But when the dehumidification system is switched off, evapotranspiration initially spiked and then began to settle towards zero as humidity began rising, the vapor pressure deficit began dropping, and as the environment approached saturation.

For reference, the dehumidification rate can also be normalized per unit of membrane surface area, which gives a range of 0.23 to 0.45 ± 0.04 g/m^2/h. These values of membrane performance are somewhat low. For example, in our previous work related to fertilizer-based liquid desiccants, we achieved vapor flux as high as 2.1 ± 0.2 g/m^2/h during

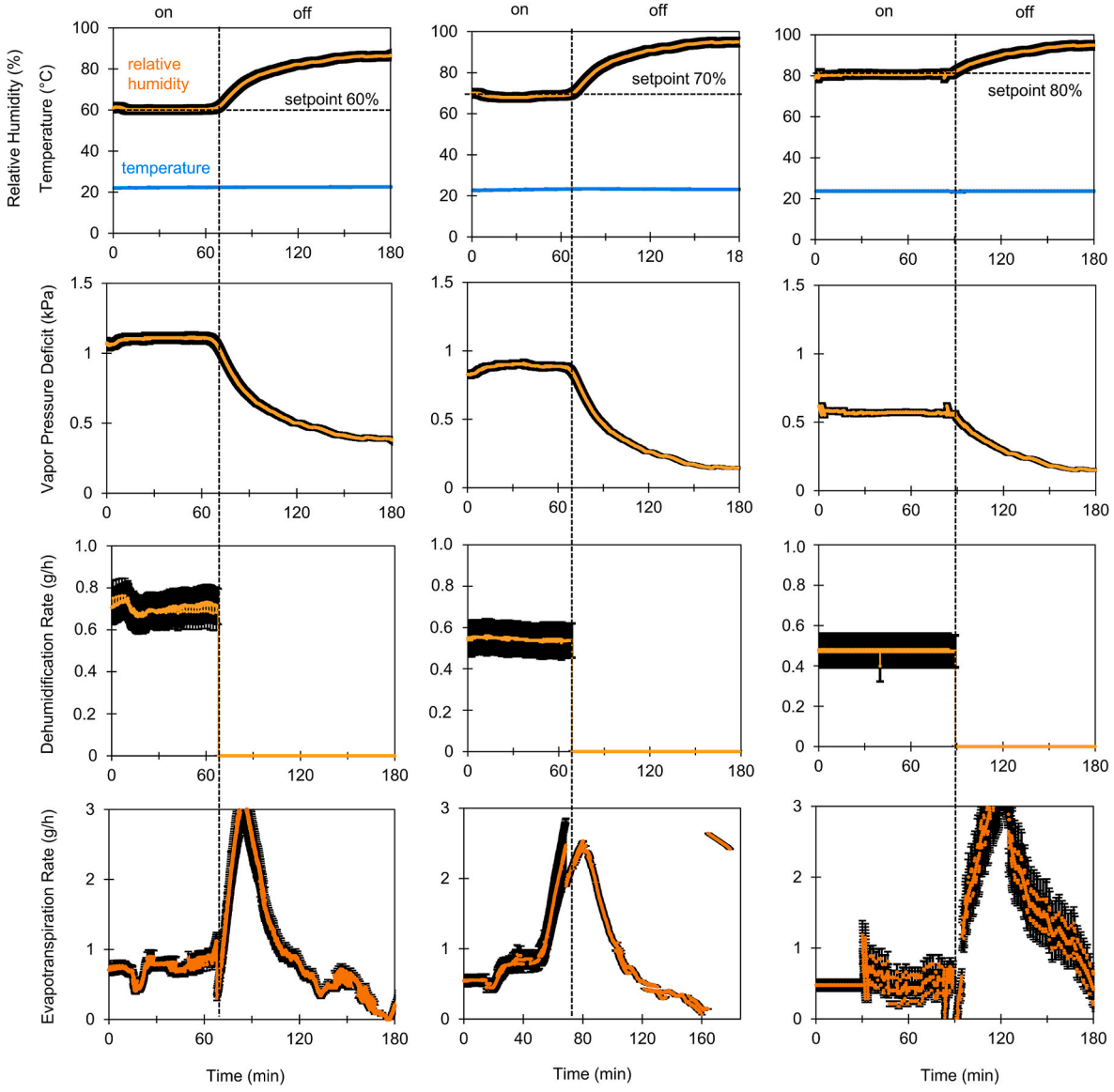

Fig. 8. Humidity, temperature, and vapor pressure deficit of the plant chamber with fully mature arugula. Humidity was initially controlled by the proposed liquid desiccant system and the dehumidification rate is observed. At ~60 min, the dehumidification system was turned off and the response of the plant chamber was observed, including the evapotranspiration rate. Complete test conditions were provided in Table 4. Supporting data is provided in Supplementary Note 3.

laboratory testing (Moussaddy et al., 2024). The reason for this low flux was that in this study, vapor flux was increased only so much as was needed to achieve the desired humidity target (this is done by controlling the liquid desiccant temperature). It is likely that flux could be further increased if desired, by adjusting operational parameters (such circulation rates, temperatures, and membrane area), but higher fluxes were unnecessary here and would only have driven humidity below the desired setpoint.

A final note, the dehumidification system does not currently have automated control, for this reason, achieving the desired set point was a matter of monitoring the humidity levels in real-time and then manually adjusting liquid desiccant temperatures in response. Proper controls can obviously be integrated in future work.

3.3. *Maintaining stable humidity throughout the complete growth cycle*

In the next round of testing, performance was evaluated over an extended period including the complete growth cycle from germination to maturity, which is approximately 36 days for hydroponic arugula. For this testing, two arugula plants were grown under conditions previously described. Calcium nitrate fertilizer was again used as liquid desiccant, but this time was prepared at lower concentrations of 25 g/l, which is closer to the fertilizer concentrations that are expected when solution is fully integrated with closed-loop plant fertigation.

Fig. 9 shows that the fertilizer desiccant system was able to successfully maintain stable humidity at the set point of 60 % rh throughout the duration of the plant's development in the chamber. Snapshots of the plants throughout the complete growth cycle are provided for reference. As shown, at the earliest stages, humidity remained relatively low and it was unnecessary to turn on the dehumidification system. Only on day 15 when plants had 5 fully formed leaves, the humidity rose above the setpoint, signaling the need for active humidity control. From this date onward, the dehumidification system was operated, initially removing 2.5 ± 0.1 g/day from day 14 to 21, and then at a much higher rate as plants further developed and evapotranspiration increased. By day 35, the dehumidification rate reached 12.4 ± 0.6 g/day. Across this range of conditions, relative humidity remained approximately stable at the 60 % setpoint.

As explained previously, the dehumidification system was not automated, therefore it was not possible to operate the system continuously for the full 36 days. Rather, it was necessary to manually operate the bench during regular business hours when it was reasonable to access the laboratory. This was done for a total of 13 out of the 23 days when dehumidification was needed (excluding the first 13 days when data was collected but no dehumidification was needed). For this reason, data in Fig. 9 is presented as discrete data points, representing the average value observed during each of the test events. Supplementary Note 4 provides supporting data for one sample day of testing, as well as the average operational results from each of the test dates.

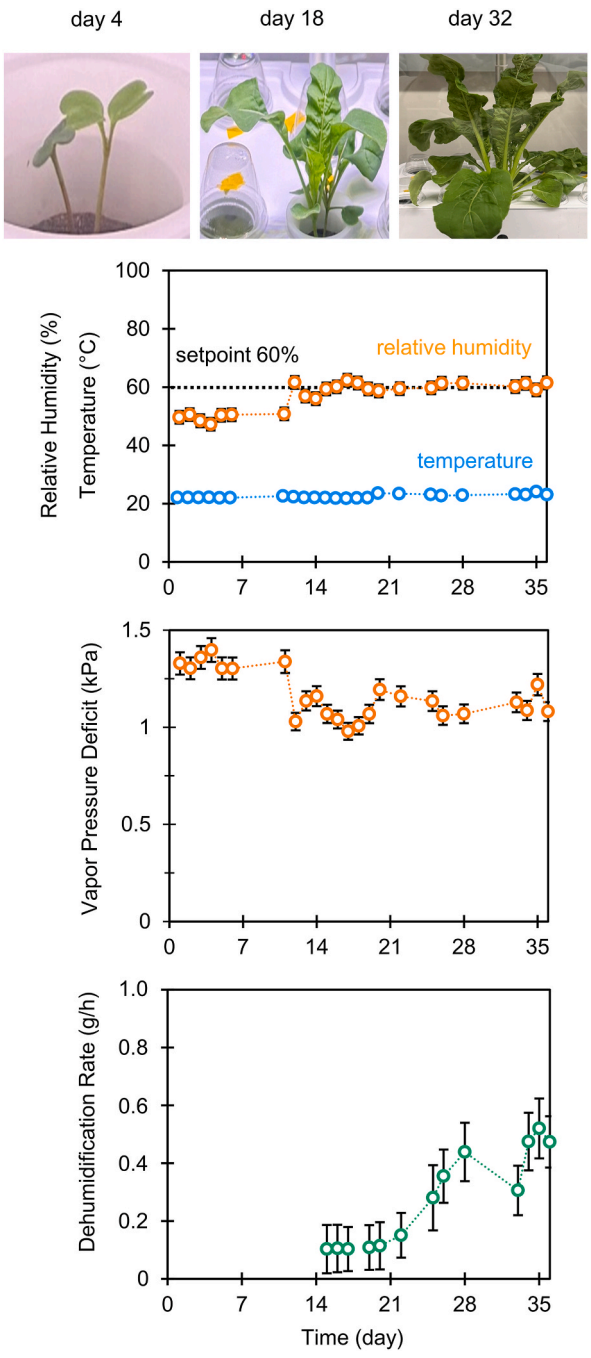

Fig. 9. Humidity, temperature, and vapor pressure deficit of the plant chamber throughout the life cycle of arugula, from germination to maturity. On day 15 humidity exceeds the 60 % rh setpoint, and the dehumidification system was activated. Dehumidification rates increased steadily to keep up with the increasing evapotranspiration rates from more mature plants. For complete test conditions see Table 4. Supporting data is provided in Supplementary Note 4, including photos of the growth progression of arugula.

4. Conclusions

This study is the first demonstration that fertilizer-based solution can be used to effectively control the humidity of a real and dynamic controlled plant environment. The plant environment consisted of a small 0.32 m^3 laboratory plant chamber, equipped with a commercial hydroponic grow system that was used to cultivate arugula. A custom liquid desiccant dehumidification apparatus with membrane contactors was built and used together with calcium nitrate solution as the fertilizer. With this setup, the possibility of using fertilizer to control humidity was studied.

In the first series of tests, it was shown that in the absence of any dehumidification, humidity of the plant environment exceeded 90 % relative humidity, and condensation on many of the surfaces of the chamber was noticeable. This was done with the hydroponic system filled to capacity with mature arugula plants, and under these conditions evapotranspiration loads reached up to 1.4 ± 0.08 g/h. In a second series of tests, the fertilizer-based dehumidification system was able to successfully control the humidity of the plant environment at desired setpoints of 60, 70, and 80 % relative humidity. By controlling the temperature of the liquid desiccant, the dehumidification rates were able to keep up with the evapotranspiration loads and thereby keep humidity stable. In this case a dehumidification rate as high as 0.76 ± 0.08 g/h was reached. In the final series of tests, the fertilizer-based dehumidification system was able to successfully maintain 60 %

relative humidity throughout all stages of the plant growth cycle, from germination to maturity, (i.e., ~36 days). Significantly, the total amount of calcium nitrate required by the arugula was sufficient to manage humidity throughout the entire growth cycle, demonstrating the system's potential for dual functionality without additional fertilizer input.

A number of limitations and priorities for future investigation have also been identified throughout the study. First, control of the liquid desiccant operating conditions, including temperature, pressure, and flow rate should be automated. This was accomplished manually in this study, but this is obviously impractical for commercial systems. Automation should also enable the implementation of more sophisticated control strategies. For example, in our previous work we have shown that energy efficiency is closely tied to operating conditions. Our focus here was simply to track the evapotranspiration load in order to maintain stable humidity, but operating an on/off duty cycle at some preferred desiccant temperature would be more energy efficient.

Second, the fertilizer-based liquid desiccant dehumidification system must be integrated with the plant fertigation system. In this study, the two were managed separately with calcium nitrate used for desiccant and a blended fertilizer used for plant nutrition. To enable this, future work must address possible fouling and precipitation risks associated with using full-formulation blended fertilizers in the dehumidification unit. These issues could be mitigated with the right buffer solution but its impact on dehumidification is yet to be investigated. Also, a few practical design modifications are needed to combine the fertilizer and desiccant circulation loops.

Third, improvements to the prototype design should be considered to enable scale up, simplify maintenance, and reduce costs. For example, the vapor flux reported in this study is relatively low, and if scaled linearly, would suggest the need for very large membrane systems at significant cost. However, this study made no effort to optimize or increase vapor flux, since instead our focus was on balancing dehumidification rates with evapotranspiration, which we achieved. In fact, increasing vapor flux beyond this point would have caused humidity to drop below the target setpoint. Future work must include design optimization that makes efficient use of the membrane surface area and dehumidification capacity. Along with this, a detailed technoeconomic analysis is needed to evaluate the cost competitiveness of the system as compared to other dehumidification technologies.In summary, this work represents the first time that fertilizer-based solution has been demonstrated to effectively control the humidity of a real and dynamic controlled plant environment. Despite certain limitations as outlined above, these results confirm the possibility of using fertilizer-based desiccant systems for integrated humidity control in indoor farming. With further development, this approach holds strong potential as a sustainable and scalable alternative for managing humidity in controlled plant environments.

CRediT authorship contribution statement

Sandeep Aryal: Writing – original draft, Visualization, Methodology, Investigation, Formal analysis, Data curation. **Foster Caragay:** Software, Methodology, Investigation, Data curation. **Danielle Monfet:** Writing – review & editing. **Mark Lefsrud:** Writing – review & editing. **Jonathan Maisonneuve:** Writing – original draft, Visualization, Validation, Methodology, Funding acquisition, Conceptualization.

Declaration of competing interest

The authors declare that they have no known competing financial interests or personal relationships that could have appeared to influence the work reported in this paper.

Acknowledgement

This material is based upon work supported by the National Science Foundation under award number 2301488. This work was also supported by the Natural Sciences and Engineering Research Council of Canada (NSERC) RGPIN-2025-05893.

Nomenclature

A	membrane surface area (m^2)
J	vapor flux (kg/s)
M	molar mass (kg/mol)
m	mass (kg)
p	pressure (Pa)
rh	relative humidity (%)
T	temperature (°C)
t	time (s)
V	volume (m^3)
VPD	vapor pressure deficit (Pa)
Greek symbols:	
ρ	density (kg/m^3)
Subscripts:	
H_2O	water vapor
sat	saturation

Appendix A. Supplementary data

Supplementary data to this article can be found online at https://doi.org/10.1016/j.jclepro.2026.147864.

Data availability

Data will be made available on request.

References

Ali, A., Ishaque, K., Lashin, A., Al Arifi, N., 2017. Modeling of a liquid desiccant dehumidification system for close type greenhouse cultivation. Energy 118, 578–589.

Amani, M., Foroushani, S., Sultan, M., Bahrami, M., 2020. Comprehensive review on dehumidification strategies for agricultural greenhouse applications. Appl. Therm. Eng. 181 (25 Nov).

Ampim, P.A.Y., Obeng, E., Olvera-Gonzalez, E., 2022. Indoor vegetable production: an alternative approach to increasing cultivation. Plants 11 (21), 2843.
Aryal, S., Caragay, F., Moussaddy, S., Lesfrud, M., Maisonneuve, J., 2025. Energy efficiency of using a novel fertilizer-based liquid desiccant system to dehumidify indoor plant environments: an experimental analysis. Energy Nexus 19, 100514.
Bahar, N.H.A., et al., 2020. Meeting the food security challenge for nine billion people in 2050: what impact on forests? Glob. Environ. Change 62, 102056.
Bettahalli, N.M.S., Lefers, R., Fedoroff, N., Leiknes, T., Nunes, S.P., 2016. Triple-bore hollow fiber membrane contactor for liquid desiccant based air dehumidification. J. Membr. Sci. 514, 135–142.
Chasseriaux, G., Travers, A., Ternoy, M., 1987. Heat pumps for reducing humidity in plastics greenhouses. Plasticulture 1987 (73), 29–40.
Cheng, J.-H., Zhang, C.-L., 2023. Capacity evaluation of mechanical dehumidification systems: a theoretical framework. Energy Convers. Manag. 310.
Cowan, N., Ferrier, L., Spears, B., Drewer, J., Reay, D., Skiba, U., 2022. CEA systems: the means to achieve future food security and environmental sustainability? Front. Sustain. Food Syst. 6 (Jun).
Cutress, D., 2021. The importance of vapor pressure deficits (VPD) in agricultural plant growth. Farm. Connect Business Wales Dec. 6.
de Halleux, D., Gauthier, L., 1998. Energy consumption due to dehumidification of greenhouses under northern latitudes. J. Agric. Eng. Res. 69, 35–42.
Fahad, F.G., Al-Humairi, S.T., Al-Ezzi, A.T., Majdi, H. Sh, Sultan, A.J., Alhuzaymi, T.M., Aljuwaya, T.M., 2023. Advancements in liquid desiccant technologies: a comprehensive review of materials, systems, and applications. Sustainability 15 (18), 14021.
Ghosh, A., Ganguly, A., 2017. Performance analysis of a partially closed solar regenerated desiccant assisted cooling system for greenhouse lettuce cultivation. Sol. Energy 158, 644–653.
Gilli, C., Kempkes, F., Munoz, P., Montero, J.I., Giuffrida, F., Baptista, F.J., Stepowska, A., Stanghellini, C., 2017. Potential of different energy saving strategies in heated greenhouse. Acta Hortic. 1170, 467–474.
Grand View Research, 2024. Indoor farming market size, share & trends analysis report by facility type, by component (hardware, software, and services), by growing mechanism, by crop category, by region, and segment forecasts, 2024–2030. Grand View Res. Rep. ID: GVR-3-68038-942-5 200 [Online]. Available: GMI1525. https://www.grandviewresearch.com.
Gurubalan, A., Simonson, C.J., 2021. A comprehensive review of dehumidifiers and regenerators for liquid desiccant air conditioning system. Energy Convers. Manag. 240, 114234.
Jain, N., et al., 2023. Global population surpasses eight billion: are we ready for the next billion? AIMS Public Health 10 (4), 849–866.
Kittas, C., Bartzanas, T., 2007. Greenhouse microclimate and dehumidification effectiveness under different ventilator configurations. Build. Environ. 42 (10), 3774–3784.
Lefers, R., Bettahalli, N.M.S., Fedoroff, N., Nunes, S.P., Leiknes, T., 2018. Vacuum membrane distillation of liquid desiccants utilizing hollow fiber membranes. Separ. Purif. Technol. 199, 57–63.
Lefers, R.M., Bettahalli, N.M.S., Fedoroff, N.V., Ghaffour, N., Davies, P.A., Nunes, S.P., Leiknes, T., 2019. Hollow fiber membrane-based liquid desiccant humidity control for controlled environment agriculture. Biosyst. Eng. 183, 47–57.
Lu, N., Nukaya, T., Kamimura, T., Zhang, D., Kurimoto, I., Takagaki, M., Maruo, T., Kozai, T., Yamori, W., 2015. Control of vapor pressure deficit (VPD) in greenhouse enhanced tomato growth and productivity during the winter season. Sci. Hortic. 197, 17–23.
Luo, J., Yang, H., 2022. A state-of-the-art review on the liquid properties regarding energy and environmental performance in liquid desiccant air-conditioning systems. Appl. Energy 325, 119853.
Lychnos, G., Davies, P.A., 2012. " Modelling and experimental verification of a solar-powered liquid desiccant cooling system for greenhouse food production in hot climates". Energy 40, 116–130.
Lysenko, E.A., Kozuleva, M.A., Klaus, A.A., Pshybytko, N.L., Kusnetsov, V.V., 2023. Lower 390 air humidity reduced both the plant growth and activities of photosystems I and II under prolonged heat stress. Plant Physiol. Biochem. 194, 246–262.
Marangoni, D.P. de O., Rezende, R., Saad, R., Hachmann, T.L., Lozano, C.S., Gonçalves, A.C.A., 2019. Water requirements and crop coefficients of arugula grown in a protected environment. IDeSCA 37 (2), 75–79.
Moussaddy, S., Pushparajah, S., Maisonneuve, J., 2022. Fertilizer-based liquid desiccants: a novel concept for energy efficient dehumidification and water vapor recycling in indoor plant environments. Appl. Therm. Eng. 218, 119529.
Moussaddy, S., Aryal, S., Maisonneuve, J., 2024. Specific energy analysis of using fertilizer-based liquid desiccants to dehumidify indoor plant environments. Appl. Therm. Eng. 238, 121849.
Naik, B.K., Joshi, M., Muthukumar, P., Sultan, M., Miyazaki, T., Shamshiri, R.R., Ashraf, H., 2020. Investigating solid and liquid desiccant dehumidification options for room air-conditioning and drying applications. Sustainability 12 (24), 10582.
Our World in Data, 2024. Breakdown of Habitable Land Area, World, 2019. OurWorldInData.org, [Online]. Available: https://ourworldindata.org/grapher/breakdown-habitable-land?time=latest. (Accessed 18 April 2025).
Penuela, J., et al., 2024. The indoor agriculture industry: a promising player in demand response services. Appl. Energy 372, 123756.
Rousse, D.R., Martin, D.Y., Thériault, R., Léveillée, F., Boily, R., 2000. Heat recovery in greenhouses: a practical solution. Appl. Therm. Eng. 20 (8), 687–706.
Sadasivam, M., Balakrishnan, A.R., 1991. Analysis of thermal effects in packed bed liquid desiccant dehumidifiers. Chem. Eng. Process. Process Intensif. 30 (2), 79–85.
Stein, E.W., 2021. The transformative environmental effects large-scale indoor farming may have on air, water, and soil. Air Soil. Water Res. 14.
Sultan, M., Miyazaki, T., Saha, B.B., Koyama, S., Maisotsenko, V.S., 2015. " Steady-state analysis on thermally driven adsorption air-conditioning system for agricultural greenhouses". Procedia Eng. 118, 185–192.
Sultan, M., Miyazaki, T., Saha, B.B., Koyama, S., 2016. " Steady-state investigation of water vapour adsorption for thermally driven adsorption based greenhouse air-conditioning system". Renew. Energy 86, 785–795.
Tibbitts, T.W., 1979. Humidity and plants. Bioscience 29 (6), 358–363.
van Dijk, M., Morley, T., Rau, M.L., Saghai, Y., 2021. A meta-analysis of projected global food demand and population at risk of hunger for the period 2010–2050. Nat. Food 2, 494–501.
Xu, J., Wei, Q., Peng, S., Yu, Y., 2012. Error of saturation vapor pressure calculated by different formulas and its effect on calculation of reference evapotranspiration in high latitude cold region. Procedia Eng. 28, 43–48.
Zeng, C., Liu, S., Shukla, A., 2017. A review on the air-to-air heat and mass exchanger technologies for building applications. Renew. Sustain. Energy Rev. 75, 753–774.